

Effectively Trainable Semi-Quantum Restricted Boltzmann Machine

Ya.S. Lyakhova^{1,2,3}*, E.A. Polyakov¹, and A.N. Rubtsov^{1,2}

¹*Russian Quantum Center, Skolkovo Innovation city, 121205 Moscow, Russia*

²*NTI Center for Quantum Communications, National University of Science and Technology MISiS, 119049 Moscow, Russia*

³*National Research Nuclear University MEPhI, 115409 Moscow, Russia*

(Dated: January 28, 2020)

We propose a novel quantum model for the restricted Boltzmann machine (RBM), in which the visible units remain classical whereas the hidden units are quantized as noninteracting fermions. The free motion of the fermions is parametrically coupled to the classical signal of the visible units. This model possesses a quantum behaviour such as coherences between the hidden units. Numerical experiments show that this fact makes it more powerful than the classical RBM with the same number of hidden units. At the same time, a significant advantage of the proposed model over the other approaches to the Quantum Boltzmann Machine (QBM) is that it is exactly solvable and efficiently trainable on a classical computer: there is a closed expression for the log-likelihood gradient with respect to its parameters. This fact makes it interesting not only as a model of a hypothetical quantum simulator, but also as a quantum-inspired classical machine-learning algorithm.

I. INTRODUCTION

Nowadays machine learning becomes an all-pervasive paradigm of how to obtain, process and store knowledge. Initially arising in the field of computer science, it finds numerous interdisciplinary applications. They range from commercial applications like speech and handwriting recognition, classification/recognition of video content [1], up to various scientific applications. As an example of the latter, in physics the most prominent applications are the generative modeling of quantum control and measurement protocols [2], and of condensed matter problems [3].

One of the major approaches to machine learning is the generative modeling. Here, given a certain finite data set X , a model of its probability distribution $P(X)$ is estimated. The tuning of the model parameters (i.e. training) is usually carried over by maximizing a certain distribution-resemblance measure. There are two criteria of a successful learning model. Firstly, it has to be easily trainable. It turns out that too complex models (or machines) are challenging and impractical to train. Stacks of simple models is a way round this problem. While each layer is easy to train, their composition can model data of high statistical complexity [4]. The second criterion is imposed by the problem of overfit. If one increases the number of model parameters for a given data set, the model tends to approximate the particular realization of the random data scatter thus losing its predictive capability. It entails that a successful machine has to be simple enough to avoid overfit.

In the classical machine learning, such a model is the Restricted Boltzmann Machine (RBM). RBM is a two-layer energy model with no coupling between the units of the same layer. One layer is called visible and represents

the observable data, while the other one is called hidden and represents some statistical correlations between the visible units. The energy of such a machine is a quadratic function of the visible and hidden variables, and their probability distribution is given by the finite-temperature Boltzmann distribution [5]. The absence of connections between the units in the same layer makes RBM a highly efficiently trainable model.

We live in the era of the second quantum revolution, which is characterized by experimental and technological achievements in the control of individual quantum systems. The major motivation behind this activity is to devise a feasible quantum computing circuits, which could outperform the capabilities of classical computing devices [6]. The field of machine learning does not stand aside. Quantum models of machine learning are being proposed [7, 8], and in particular, recently the quantum Boltzmann machine (QBM) was proposed [9]. The main difference from the classical Boltzmann machine is that both the visible and hidden units (spins) are allowed to be in a state of quantum superposition. The energy function (Hamiltonian) is modified to include a non-diagonal connections of spins to an external field (bias). While such a model is demonstrated to learn the data distribution better than the classical RBM, its major drawback is that this model is of high computational complexity, and its training is challenging.

The purpose of this work is to present a quantum version of the Restricted Boltzmann Machine, which at the same time has reasonable computational complexity so that it can be efficiently trained. We propose to represent the hidden units by non-interacting fermions. Technically it amounts to the replacement of a vector of m hidden units with quadratic matrix of the size $m \times m$, and thus hidden bias and coupling between the layers are now represented by $m \times m$ matrix and $n \times m \times m$ -matrix respectively, with n visible units. Analogously to the classical RBM, where the coupling between the layers is linear, the free-motion Hamiltonian for the fermionic

* yanalyakhova@gmail.com

hidden units is linearly coupled to the visible (classical) units. We call it the semi-quantum Restricted Boltzmann Machine (sqRBM).

We evaluate the proposed sqRBM model on the two training data sets: the ensemble of Bars&Stripes [10], and the Optdigits dataset of the handwritten digits [11]. We compare the log-likelihood with the classical RBM. Also we present the results of the cross-validation test to compare the overfit of sqRBM and RBM.

In the Section 2 we briefly overview the RBM model and its training procedures. Section 3 is devoted to the detailed description of the proposed semi-quantum RBM. In this case the probability distribution is given in terms of density matrix, and the usual summation over the classical hidden units is replaced with the taking of trace w.r.t. quantum fermionic hidden units. We also derive learning rules for the training via gradient ascent algorithm, and discuss the numerical implementation in details. We show the results of numerical experiments in the Section 4, where we conduct tests using Bars&Stripes set and OptDigits set as the input training data. Our conclusions are set out in the Section 5.

II. CLASSICAL RESTRICTED BOLTZMANN MACHINE

A. Model

Restricted Boltzmann Machine (RBM) is a bipartite undirected neural network (see Fig. 1a). One of its layers is conventionally called visible and the other one hidden (see Fig. 1b). Both visible (\mathbf{v}) and hidden (\mathbf{h}) neurons are assumed to take the values $\{0, 1\}$. The former is used to describe the observable data, whereas the latter is used to model the correlations between the observable components.

RBM is an energy-based model, which dynamics can be described by the Gibbs-Boltzmann distribution:

$$p(\mathbf{v}, \mathbf{h}) = \frac{1}{Z} e^{-E(\mathbf{v}, \mathbf{h})}, \quad (1)$$

with the conventional definition of partition function

$$Z = \sum_{\mathbf{v}} \sum_{\mathbf{h}} e^{-E(\mathbf{v}, \mathbf{h})}. \quad (2)$$

Physically it corresponds to the assumption that RBM system is in the thermal equilibrium at the finite temperature $1/T = 1$. The energy $E(\mathbf{v}, \mathbf{h})$ of the machine is postulated to be a quadratic function of its variables. For the RBM of m visible units and n hidden ones we have

$$E(\mathbf{v}, \mathbf{h}) = - \sum_{i=1}^m b_i v_i - \sum_{j=1}^n c_j h_j - \sum_{i=1}^m \sum_{j=1}^n v_i w_{ij} h_j. \quad (3)$$

Here, coefficients \mathbf{b} and \mathbf{c} are called biases, whereas \mathbf{w} is a weight matrix.

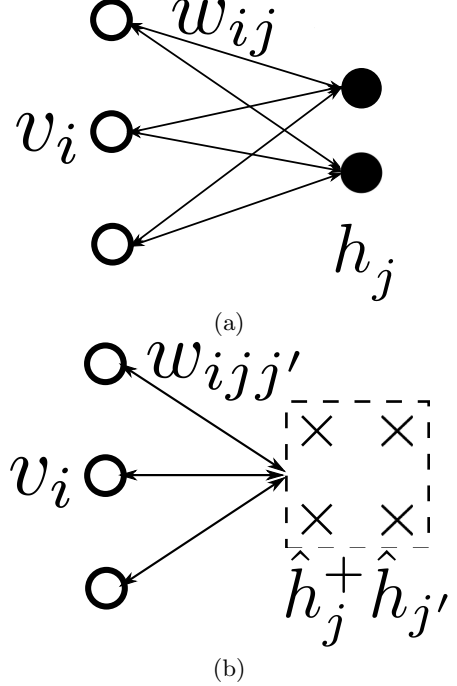


FIG. 1. RBM (a) and sqRBM (b) schemes. They consist of two interacting layers, one of which is called visible v_i and the other one hidden. Dimensionality of sqRBM hidden layer $\hat{h}_j \hat{h}'_j$ is twice the dimensionality of the corresponding RBM hidden layer h_j . The interaction between the layers is denoted with w_{ij} for the RBM and with $w_{ijj'}$ for the sqRBM.

The absence of connections between the units of the same layer of RBM allows one to treat their states as mutually independent in terms of probability, namely [12]

$$p(\mathbf{h}|\mathbf{v}) = \prod_{j=1}^m p(h_j|\mathbf{v}), \quad (4)$$

and vice versa. This property makes RBM solvable and effectively trainable model via the method of direct Gibbs sampling [13].

B. Training

The main idea of RBM usage is to model the distribution of observable data $p^{data}(\mathbf{v})$. This is achieved by the adjustment of the biases \mathbf{b}, \mathbf{c} and weights \mathbf{w} (the parameters of the model) so that the marginal distribution of the visible layer $p(\mathbf{v})$ would be as close as possible to the target distribution $p^{data}(\mathbf{v})$.

The measure of target and model distributions proximity can be represented by the log-likelihood function

$$\mathcal{L}(\mathbf{b}, \mathbf{c}, \mathbf{w}) = \frac{1}{N_{data}} \sum_{\mathbf{v}_{data}} \log p(\mathbf{v}_{data}). \quad (5)$$

The higher $\mathcal{L}(\mathbf{b}, \mathbf{c}, \mathbf{w})$ the better given RBM models the observables' distribution.

Maximizing the log-likelihood \mathcal{L} (or equivalently minimizing the negative log-likelihood $-\mathcal{L}$) can be implemented by the gradient ascent (descent) algorithm [5]. It can be shown [12] that it gives the following update rules for biases and weights:

$$\begin{aligned}\Delta \mathbf{b} &= \eta \partial_{\mathbf{b}} \mathcal{L}(\mathbf{b}, \mathbf{c}, \mathbf{w}) = \\ &= \eta \left(\frac{1}{N_{data}} \sum_{\mathbf{v}_{data}} \mathbf{v}_{data} - \sum_{\mathbf{v}} P(\mathbf{v}) \mathbf{v} \right),\end{aligned}\quad (6a)$$

$$\begin{aligned}\Delta \mathbf{c} &= \eta \partial_{\mathbf{c}} \mathcal{L}(\mathbf{b}, \mathbf{c}, \mathbf{w}) = \\ &= \eta \left(\frac{1}{N_{data}} \sum_{\mathbf{v}_{data}, \mathbf{h}} P(\mathbf{v}_{data}, \mathbf{h}) \mathbf{h} \right. \\ &\quad \left. - \sum_{\mathbf{v}, \mathbf{h}} P(\mathbf{v}, \mathbf{h}) \mathbf{h} \right),\end{aligned}\quad (6b)$$

$$\begin{aligned}\Delta \mathbf{w} &= \partial_{\mathbf{w}} \mathcal{L}(\mathbf{b}, \mathbf{c}, \mathbf{w}) = \\ &= \eta \left(\frac{1}{N_{data}} \sum_{\mathbf{v}_{data}, \mathbf{h}} P(\mathbf{v}_{data}, \mathbf{h}) \mathbf{v}_{data} \mathbf{h} - \right. \\ &\quad \left. - \sum_{\mathbf{v}, \mathbf{h}} P(\mathbf{v}, \mathbf{h}) \mathbf{v} \mathbf{h} \right).\end{aligned}\quad (6c)$$

Here η is called learning rate and defines the size of a single gradient ascent step.

There are various techniques of how to actually evaluate the gradients (6). In this work we employ the fast mean-field-like algorithm called Contrastive Divergence (CD) [13], and the full Monte-Carlo simulation called Persistent Contrastive Divergence (PCD) [14].

III. SEMI-QUANTUM RESTRICTED BOLTZMANN MACHINE

A. Model

In the semi-quantum case we propose a two-layer system again (see Fig. 1b). The visible layer is the same as in the case of a classical RBM. Its units are classical binary variables \mathbf{v} . On the contrary, the hidden layer is composed of quantum degrees of freedom $\hat{\mathbf{h}}$. In the spirit of Schwinger-Wigner representation each hidden binary unit is represented by a pair of fermionic creation/annihilation operators. Such a system is described by the following Hamiltonian:

$$\begin{aligned}\hat{H}(\mathbf{v}, \mathbf{h}) &= - \sum_{i=1}^n b_i v_i - \sum_{j,j'=1}^m c_{jj'} \hat{h}_j^+ \hat{h}_{j'} \\ &\quad - \sum_{i=1}^n \sum_{j,j'=1}^m v_i w_{ijj'} \hat{h}_j^+ \hat{h}_{j'},\end{aligned}\quad (7)$$

where \mathbf{c} is a Hermitian matrix and $w_{ijj'}$ is a Hermitian matrix w.r.t. j, j' for a given i . We call this model Semi-Quantum Restricted Boltzmann Machine (sqRBM).

As in the classical case we assume that sqRBM is in the state of thermal equilibrium at some finite inverse temperature β . Thus its state is described by the canonical ensemble in terms of the density matrix

$$\hat{\rho}(\mathbf{v}, \mathbf{h}) = \frac{e^{-\beta \hat{H}(\mathbf{v}, \mathbf{h})}}{Z}.\quad (8)$$

Here the partition function Z of this hybrid classical-quantum system is given by

$$Z = \sum_{\mathbf{v}} \text{Tr}_h(e^{-\beta \hat{H}(\mathbf{v}, \mathbf{h})}),\quad (9)$$

where $\sum_{\mathbf{v}}$ stands for the ordinary summation over the observable classical \mathbf{v} , and the trace Tr_h is taken over the quantum hidden degrees of freedom. Hereinafter we set $\beta = 1$ for simplicity.

Fermionic hidden subsystems obeys the Fermi-Dirac statistics:

$$p(\hat{h}_j^+ \hat{h}_{j'} | \mathbf{v}) = \left(\frac{1}{1 + e^{-H_h}} \right)_{jj'},\quad (10)$$

where $H_h = -c_{jj'} - \sum_{i=1}^n v_i w_{ijj'}$ is a $m \times m$ matrix. It is clear now that in the case when the Hamiltonian (7) is diagonal in the fermionic degrees of freedom, namely $c_{jj'} = c_{jj} \delta_{jj'}$ and $w_{ijj'} = w_{ijj} \delta_{jj'}$, it is fully equivalent to the classical RBM (3).

B. Training

As in the case of classical RBM the goal of training is to approximate the probability distribution of data $p^{data}(\mathbf{v})$ by the marginal probability distribution $p(\mathbf{v})$ of visible variables

$$p^{data}(\mathbf{v}) \approx p(\mathbf{v}) = \frac{Z_v}{Z},\quad (11)$$

where $Z_v(\mathbf{b}, \mathbf{c}, \mathbf{w})$ is the conditional partition function (see eq. (9))

$$\begin{aligned}Z_v(\mathbf{b}, \mathbf{c}, \mathbf{w}) &= \text{Tr}_h e^{-\hat{H}} = \\ &= e^{\mathbf{b}\mathbf{v}} \text{Tr} \exp \sum_{j,j'=1}^m (c_{jj'} + \sum_{i=1}^n v_i w_{ijj'}) \hat{h}_j^+ \hat{h}_{j'} = \\ &= e^{\mathbf{b}\mathbf{v}} \det(\mathbf{1} + e^{H_h}),\end{aligned}\quad (12)$$

and H_h is introduced in (10). For this purpose we adjust the model parameters $\mathbf{b}, \mathbf{c}, \mathbf{w}$ so that the log-likelihood of the data set \mathbf{v}_{data} would be maximum for a given set of model parameters (see Eq. (5)). To maximize the log-likelihood we use the gradient ascent algorithm again:

$$\Delta \mathbf{b} = \eta \partial_{\mathbf{b}} \mathcal{L}(\mathbf{b}, \mathbf{c}, \mathbf{w}),\quad (13a)$$

$$\Delta \mathbf{c} = \eta \partial_{\mathbf{c}} \mathcal{L}(\mathbf{b}, \mathbf{c}, \mathbf{w}), \quad (13b)$$

$$\Delta \mathbf{w} = \eta \partial_{\mathbf{w}} \mathcal{L}(\mathbf{b}, \mathbf{c}, \mathbf{w}). \quad (13c)$$

The ascent step for the visible bias \mathbf{b} coincides with that of RBM (6), as far as the visible subsystem is postulated to be purely classical. Consider now the ascent step for the hidden bias \mathbf{c} :

$$\begin{aligned} \partial_{\mathbf{w}} \mathcal{L}(\mathbf{b}, \mathbf{c}, \mathbf{w}) &= \frac{1}{N_{data}} \sum_{\mathbf{v}_{data}} (\partial_{\mathbf{w}} \log Z_{v_{data}} - \partial_{\mathbf{w}} \log Z) = \\ &= \frac{1}{N_{data}} \sum_{\mathbf{v}_{data}} \left(Z_{v_{data}}^{-1} \partial_{\mathbf{w}} Z_{v_{data}} \right. \\ &\quad \left. - Z^{-1} \sum_{\mathbf{v}} \partial_{\mathbf{w}} Z_{v_{data}} \right). \end{aligned} \quad (14)$$

Let us evaluate separately the gradient of $Z_{v_{data}}$. Here and in the following we omit the subscript *data* during this calculation for simplicity:

$$\begin{aligned} \partial_{\mathbf{w}} Z_v &= e^{\mathbf{b}\mathbf{v}} \partial_{\mathbf{w}} \det(\mathbf{1} + e^{H_h}) = \\ &= e^{\mathbf{b}\mathbf{v}} \text{Tr}(\det(\mathbf{1} + e^{H_h}) \cdot (1 + e^{H_h})^{-1} \partial_{\mathbf{w}} (\mathbf{1} + e^{H_h})) = \\ &= Z_v \text{Tr}(p(\mathbf{h}^+ \mathbf{h} | \mathbf{v}) \mathbf{v} \mathbf{h}^+ \hat{\mathbf{h}}). \end{aligned} \quad (15)$$

Substituting this into (14) and assuming that there are N_{data} samples of visible units in the input dataset, we obtain

$$\begin{aligned} \partial_{\mathbf{w}} \mathcal{L}(\mathbf{b}, \mathbf{c}, \mathbf{w}) &= \frac{1}{N_{data}} \sum_{\mathbf{v}_{data}} \text{Tr}[p(\mathbf{v}_{data}, \mathbf{h}^+ \mathbf{h}) \mathbf{v}_{data} \mathbf{h}^+ \mathbf{h}] \\ &\quad - \sum_{\mathbf{v}} \text{Tr}[p(\mathbf{v}, \mathbf{h}^+ \mathbf{h}) \mathbf{v} \mathbf{h}^+ \mathbf{h}]. \end{aligned} \quad (16)$$

For the gradient w.r.t. the hidden layer bias \mathbf{c} one can proceed in the same way to obtain

$$\begin{aligned} \partial_{\mathbf{c}} \mathcal{L}(\mathbf{b}, \mathbf{c}, \mathbf{w}) &= \frac{1}{N_{data}} \sum_{\mathbf{v}_{data}} \text{Tr}[p(\mathbf{v}_{data}, \mathbf{h}^+ \mathbf{h}) \mathbf{h}^+ \mathbf{h}] \\ &\quad - \sum_{\mathbf{v}} \text{Tr}[p(\mathbf{v}, \mathbf{h}^+ \mathbf{h}) \mathbf{h}^+ \mathbf{h}]. \end{aligned} \quad (17)$$

The update of the biases \mathbf{b} , \mathbf{c} and weights \mathbf{w} is proportional to the relative gradients with the proportionality factor η , which is the learning rate.

C. Gibbs sampling

During the training of both classical RBM and sqRBM one needs to evaluate the mean values of different quantities namely visible units, hidden units and their combination. In practice it can be implemented by generating a large amount (representative set) of samples with some underlying probability distribution, which is not known explicitly, and then by taking the mean value over the generated samples. To do so one may apply the so-called

Gibbs sampling [12], which allows to produce samples from some joint probability distribution (\mathbf{v}, \mathbf{h}) . Basically it allows us to update the state of visible layer \mathbf{v} for a given hidden layer state \mathbf{h} and vice versa. This procedure is applicable and quite efficient because all hidden units are independent of each other, and the same for the visible ones.

During the training of an sqRBM though we cannot apply Gibbs sampling straightforwardly. This is because of the introduction of a $m \times m$ matrix for the hidden layer instead of a m -dimensional vector with mutually independent components. In this case diagonalization can fix the problem. One has to include this step into the usual Gibbs sampling algorithm. Update of the visible layer for a given hidden state stays the same as for the classical RBM.

To sum up we suggest the following pseudo-code for the numerical realization of sqRBM [5, 12]:

Here \mathbf{E} is the number of descent steps; \mathbf{K} is the number of Gibbs sampling steps; $\sigma_{el/m}$ is the element-wise/matrix logistic (sigma) function; $sample[\dots]$ is the stochastic turn on of visible neuron with the probability $[\dots]$; $\Delta \dots$ is the increment of the corresponding quantity which is proportional to r.h.s. with the coefficient of proportionality equal to the learning rate.[15]

D. Persistent Contrastive Divergence

The exact evaluation of the gradient in eq. (13) can be achieved by the Monte Carlo simulation. The positive part of the gradient involves the averaging of the single-particle density matrix (10) and its moments over the training data points \mathbf{v}_{data} . The negative part of the gradient involves the averaging of the same quantities over \mathbf{v} with the model probability $p(\mathbf{v})$. The latter requires to perform a separate Monte Carlo simulation via the Metropolis algorithm [16] for each gradient ascent step which is impractical. The way out is provided by the observation that when the learning rate η is small, the

TABLE I. Pseudo-code of Training for sqRBM

1. Initialization of machine: $\mathbf{W} \leftarrow gauss(\mu = 0, \sigma = 0.01)$ $\mathbf{a}, \mathbf{b} \leftarrow (0 \dots 0)$
2. Training procedure:
For \mathbf{e} in $(1 \dots \mathbf{E})$ do :
$\mathbf{v}^0 \leftarrow (training \ set)$
$(\mathbf{h}^+ \mathbf{h})^0 \leftarrow \sigma_m(\mathbf{v}^0 \cdot \mathbf{W} + \mathbf{b})$
For \mathbf{k} in $(1 \dots \mathbf{K})$ do :
Diagonalization $[(\mathbf{h}^+ \mathbf{h})^{k-1}]$
$\mathbf{v}^k \leftarrow sample[\sigma_{el}((\mathbf{h}^+ \mathbf{h})^{k-1} \cdot \mathbf{W} + \mathbf{a})]$
$(\mathbf{h}^+ \mathbf{h})^k \leftarrow \sigma_m(\mathbf{v}^k \cdot \mathbf{W} + \mathbf{b})$
$\Delta \mathbf{W} \sim \langle \mathbf{v} \mathbf{h}^+ \mathbf{h} \rangle^0 - \langle \mathbf{v} \mathbf{h}^+ \mathbf{h} \rangle^k$
$\Delta \mathbf{a} \sim \langle \mathbf{v} \rangle^0 - \langle \mathbf{v} \rangle^k$
$\Delta \mathbf{b} \sim \langle \mathbf{h}^+ \mathbf{h} \rangle^0 - \langle \mathbf{h}^+ \mathbf{h} \rangle^k$

model is changed only slightly, so that we can continue the Markov Chain from the state at the previous learning step. Provided that the change of η is sufficiently small between the steps, such a chain will follow close enough the probability distribution of the model at the current set of parameters. In other words, we perform a single Metropolis simulation of the model. At each Monte Carlo step the negative part of the gradient is approximated by its value for the current configuration of the model. The positive part of the gradient is estimated by drawing a random training data point \mathbf{v}_{data} at each Monte Carlo step. Then the model parameters are updated according to (13). This is called the Persistent Chain (PC) [14]. However the fluctuations of the gradient estimate may hinder the convergence of the gradient-ascent procedure. In order to reduce these fluctuations, one simulates not one but several independent concurrent Persistent Chains, and the increment of model parameters is averaged over the chains. This is called the Persistent Contrastive Divergence algorithm.

IV. TESTS

We perform the comparative observations of RBM and sqRBM by training the machines on two familiar datasets. The first one is a set of 4×4 square pic-

TABLE II. Pseudo-code of Persistent Contrastive Divergence Training Procedure for sqRBM

1. Initialization of machine:
 $\mathbf{W} \leftarrow gauss(\mu = 0, \sigma = 0.01)$
 $\mathbf{b}, \mathbf{c} \leftarrow (0 \dots 0)$
For \mathbf{i} in $(1 \dots N_{pcd})$ do :
 $\mathbf{v}_{pcd}^0[\mathbf{i}] \leftarrow (vector\ of\ random\ bits)$
 $\mathbf{W}_{pcd}^0[\mathbf{i}] \leftarrow p(\mathbf{v}_{pcd}^0[\mathbf{i}])$
2. Training procedure:
For e in $(1 \dots E)$ do :
 $\Delta \mathbf{W} = 0$
 $\Delta \mathbf{a} = 0$
 $\Delta \mathbf{b} = 0$
 $\mathbf{v}_{data} \leftarrow (random\ instance\ of\ training\ set)$
 $(\mathbf{h}^+ \mathbf{h})_{data} \leftarrow \sigma_m (\mathbf{v}_{data} \cdot \mathbf{W} + \mathbf{b})$
For \mathbf{i} in $(1 \dots N_{pcd})$ do :
 $\mathbf{v}_{trial} \leftarrow (generate\ trial\ configuration\ from\ \mathbf{v}_{pcd}^{e-1}[\mathbf{i}])$
 $\mathbf{W}_{trial} \leftarrow p(\mathbf{v}_{trial})$
If \mathbf{v}_{trial} is accepted based on Metropolis rule
 for $\mathbf{W}_{trial}/\mathbf{W}_{pcd}^{e-1}[\mathbf{i}]$ then $\mathbf{v}_{pcd}^e[\mathbf{i}] \leftarrow \mathbf{v}_{trial}$
Else
 $\mathbf{v}_{pcd}^e[\mathbf{i}] \leftarrow \mathbf{v}_{pcd}^{e-1}[\mathbf{i}]$
 $(\mathbf{h}^+ \mathbf{h})_{pcd}[\mathbf{i}] \leftarrow \sigma_m (\mathbf{v}_{pcd}^e[\mathbf{i}] \cdot \mathbf{W} + \mathbf{b})$
 $\Delta \mathbf{W} = \Delta \mathbf{W} + \mathbf{v}_{data}(\mathbf{h}^+ \mathbf{h})_{data} - \mathbf{v}_{pcd}^e[\mathbf{i}] (\mathbf{h}^+ \mathbf{h})_{pcd}[\mathbf{i}]$
 $\Delta \mathbf{a} = \Delta \mathbf{a} + \mathbf{v}_{data} - \mathbf{v}_{pcd}^e[\mathbf{i}]$
 $\Delta \mathbf{b} = \Delta \mathbf{b} + (\mathbf{h}^+ \mathbf{h})_{data} - (\mathbf{h}^+ \mathbf{h})_{pcd}[\mathbf{i}]$
 $\mathbf{W} \leftarrow \mathbf{W} + \eta \Delta \mathbf{W}$
 $\mathbf{a} \leftarrow \mathbf{a} + \eta \Delta \mathbf{a}$
 $\mathbf{b} \leftarrow \mathbf{b} + \eta \Delta \mathbf{b}$

tures with random black-and-white *Bars&Stripes* (see Fig. 2a). The second one is *OptDigits* [11] (see Fig. 3a). This is a set of 5620 8×8 originally grayscale samples of handwritten digits, which we simplified to black-and-white ones (see Fig. 3). In each test the number of visible neurons was fixed to the number of pixels in one image.

A. Training by Contrastive Divergence

The first experiment was conducted in order to compare the performances of RBM and sqRBM with use of simple Contrastive Divergence algorithm with one Gibbs sampling step (CD_1). The measure of training quality was the log-likelihood of the training data set. For estimating the log-likelihood we used annealed importance sampling (AIS) [17]. During the experiment the learning rate followed the search-then-converge rule [18]: $\eta(n) = \eta_0/(1 + n/n_0)$, where η_0 is the starting learning rate, n is the number of current step, and n_0 is the decrease parameter. For the training on both datasets we used $\eta_0 = 0.1$, $n_0 = 300$. In this experiment we trained a RBM with 9 hidden units and a sqRBM with 3 hidden units on the Bars&Stripes set, and a RBM with 36 and a sqRBM with 6 hidden units on the OptDigits set. The results are presented on Fig. 2 and 3. Sharp peaks and following slump of the log-likelihood is the typical behaviour for CD_1 algorithm [12]. Increase in the number of Gibbs steps eliminates this slump as it can be seen further. It can be seen that for both Bars&Stripes and OptDigits sets sqRBM demonstrate better results than RBM.

B. Training by Persistent Contrastive Divergence

In Fig. 4 the results of training RBM and sqRBM on the 4×4 Bars&Stripes dataset are presented. It shows that making the hidden units quantum leads to significant improvement of the learning capabilities of the model. sqRBM was trained with the constant learning rate $\eta = 0.001$. In the case of RBM, $\eta = 0.001$ for the number of hidden units ≤ 5 , and $\eta = 0.0001$ for higher number of hidden units. In all cases the minibatch size (number of concurrent PC) is 100. The training dataset was 40000 random instances of the Bars&Stripes.

In Fig. 5 the results of training of RBM and sqRBM on the Optdigits dataset are presented. In all the cases $\eta = 0.001$ was employed. The minibatch size is 100. Here we also observe the improvement due to the quantumness of the hidden units. The convergence rate of sqRBM is also faster than of RBM.

We conclude with the observation that sqRBM with N quantum hidden units tends to learn better than the RBM with N^2 classical hidden units

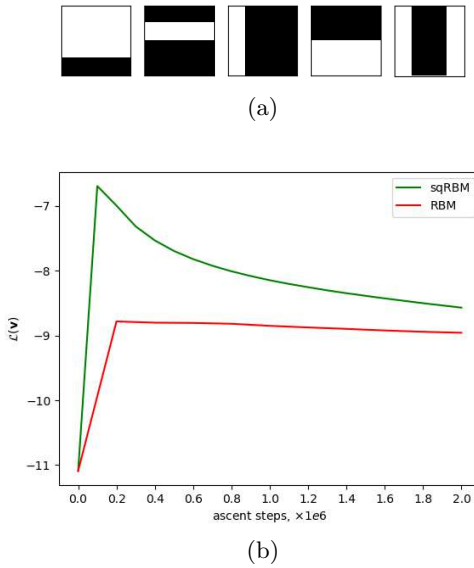


FIG. 2. Log-likelihood vs. the number of ascent steps (b) for the training on the set of bars and stripes (a). Training comparison for RBM and sqRBM.

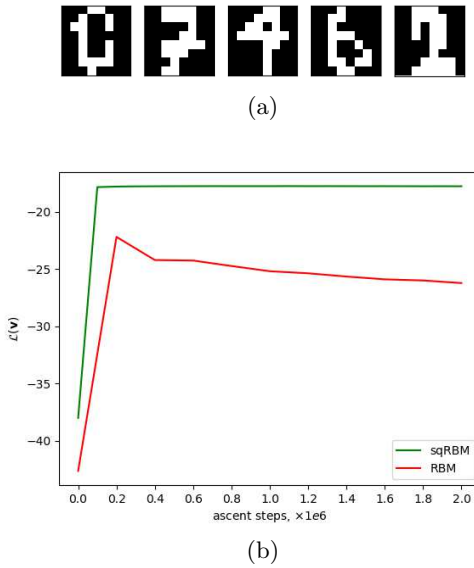


FIG. 3. Log-likelihood vs. the number of ascent steps (b) for the training on the OptDigits set (a). Training comparison for RBM and sqRBM.

C. Overfit

The overfit (i.e. degradation of the predictive capability of the model) may be estimated as the drop of likelihood when the model is shown the data which it did not see before. In Fig. 6 we present the results of such a calculation. The Optdigits dataset was partitioned into the training subset, which was chosen as the first 2800 samples. Next 5600 samples were considered as the validating subset. The models (RBM and sqRBM) learned

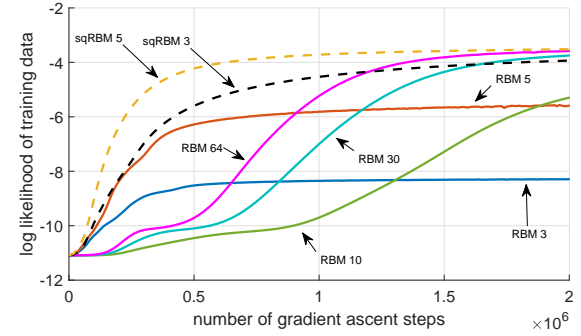


FIG. 4. Modelling the 4x4 Bars&Stripes dataset with RBM and sqRBM at different numbers of hidden units. The type of model and the number of hidden units are indicated by arrows.

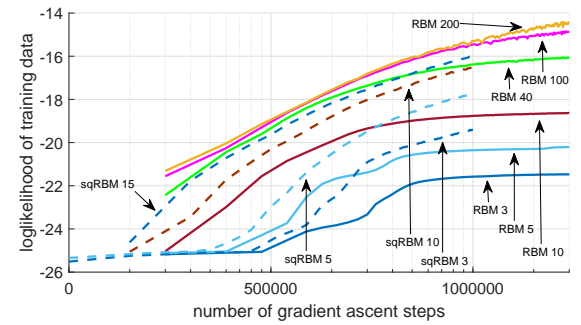


FIG. 5. Modelling the Optdigits dataset with RBM and sqRBM at different numbers of hidden units. The type of model and the number of hidden units are indicated by arrows.

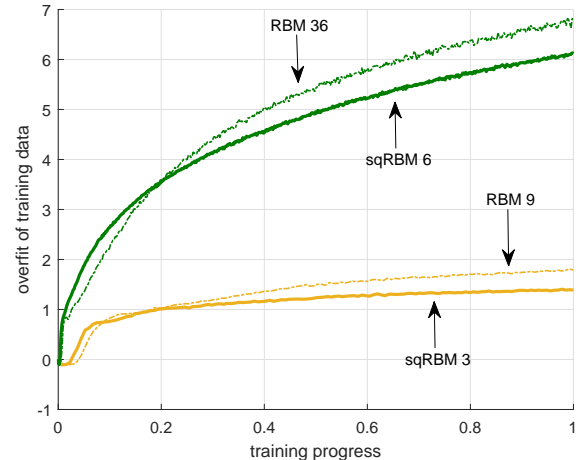


FIG. 6. Overfit of the RBM and sqRBM models on the Optdigits dataset. The "training progress" are the gradient ascent steps up to the saturation of log-likelihood on the training data. The step numbers are normalized to be 1 at the point of saturation of the training log-likelihood.

on the training subset. The log-likelihood of the training subset was calculated. Then the log-likelihood of the validating subset was calculated. The amount by which the log likelihood of the validating subset decreases is the measure of the overfit: the higher the worse. In Fig. 6 we present the overfits of sqRBM and of RBM model with a quadratically larger number of hidden units (see the end of the previous section), as a function of the training progress. The latter is defined as follows. As the models are trained, the log-likelihood first starts to grow then saturates at a certain level (i.e. the model no longer learns from the training dataset). As the saturation is achieved, the training is stopped. This corresponds to a certain (maximal) number of gradient ascent steps. For each model, we "normalize" the training progress by dividing the current number of the gradient ascent step by the maximal number before saturation. We see that sqRBM is slightly better than RBM.

V. CONCLUSION

We proposed and examined a semi-quantum version of the Restricted Boltzmann Machine with classical visible

units and fermionic hidden units which we called semi-quantum RBM (sqRBM). The presented sqRBM model inherits simple and effective trainability of the classical RBM. In particular this model can be trained using the Gibbs sampling with including diagonalization w.r.t. the hidden units as an additional step.

At the same time introduction of quantum hidden degrees of freedom makes the model sufficiently more flexible than the purely classical one. Moreover sqRBM avoid overfit better than the classical RBM. It was confirmed during the numerical experiments with the use of two standard data sets, namely Bars&Stripes and OptDigits. As a performance measure we used the log-likelihood estimation via annealed importance sampling. Future work should investigate whether this success stays for larger data sets.

The distinctive features of our model (hybrid classical/quantum system and fermionic quantum part) makes it an interesting interesting option for the development of quantum-inspired machine learning algorithms.

[1] G. W. Taylor, G. E. Hinton, and S. T. Roweis, Modeling human motion using binary latent variables, in *Advances in Neural Information Processing Systems 19 (NIPS 2006)* (MIT Press, 2006).

[2] M. Y. Niu, S. Boixo, and V. N. Smelyanskiy, Universal quantum control through deep reinforcement learning, *npj Quantum Inf* **5**, 33 (2019).

[3] J. Carrasquilla and R. Melko, Machine learning phases of matter, *Nature Phys* **13**, 431 (2017).

[4] Y. LeCun, Y. Bengio, and G. Hinton, Deep learning, *Nature* **521**, 436 (2015).

[5] G. E. Hinton, A practical guide to training restricted boltzmann machines, in *Neural Networks: Tricks of the Trade. Lecture Notes in Computer Science*, Vol. 7700, edited by M. G., O. G.B., and M. KR. (Springer, Berlin, Heidelberg, 2012) pp. 599–619.

[6] M. A. Nielsen and I. Chuang, *Quantum Computation and Quantum Information* (Cambridge University Press, Cambridge, UK, 2002).

[7] P. Rebentrost, M. Mohseni, and S. Lloyd, Quantum support vector machine for big data classification, *Phys. Rev. Lett.* **113**, 130503 (2014).

[8] P. Rebentrost, T. R. Bromley, C. Weedbrook, and S. Lloyd, Quantum hopfield neural network, *Phys. Rev. A* **98**, 042308 (2018).

[9] M. H. Amin, E. Andriyash, J. Rolfe, B. Kulchytskyy, and R. Melko, Quantum boltzmann machine, *Phys. Rev. X* **8**, 021050 (2018).

[10] A. Fischer and C. Igel, Empirical analysis of the divergence of gibbs sampling based learning algorithms for restricted boltzmann machines, in *Proceedings of Artificial Neural Networks - ICANN 2010 - 20th International Conference* (2010) pp. 208 – 217.

[11] C. Alpaydin, E. Kaynak, *Optical Recognition of Handwritten Digits* (1998), <https://www.openml.org/d/28>.

[12] A. Fischer and C. Igel, An Introduction to Restricted Boltzmann Machines, *Progress in Pattern Recognition, Image Analysis, Computer Vision, and Applications. CIARP 2012. Lecture Notes in Computer Science* **7441**, 14 (2012).

[13] G. Hinton, Training Products of Experts by Minimizing Contrastive Divergence, *Neural Computation* **14**(8), 1711 (2002).

[14] T. Tieleman, Training restricted boltzmann machines using approximations to the likelihood gradient, in *ICML'08: Proceedings of the 25th international conference on Machine learning* (ACM, 2008) pp. 1064 – 1071.

[15] J. Hopfield, Neural Networks and Physical Systems with Emergent Collective Computational Abilities, *Proceedings of the National Academy of Sciences* **79**, 2554 (1982).

[16] W. K. Hastings, Monte Carlo sampling methods using Markov chains and their applications, *Biometrika* **57**, 97 (1970).

[17] R. Neal, Annealed Importance Sampling, *Statistics and Computing* **11**, 125 (2001).

[18] K. Cho, T. Raiko, and A. Ilin, Parallel tempering is efficient for learning restricted boltzmann machines, in *The 2010 International Joint Conference on Neural Networks (IJCNN)* (IEEE, 2010) pp. 1 – 8.